Microwave Zeeman Spectrum of Atomic Oxygen*†

H. E. RADFORD‡ AND V. W. HUGHES
Gibbs Physics Laboratory, Yale University, New Haven, Connecticut
(Received December 1, 1958)

The technique of paramagnetic resonance absorption has been used to measure the g-factors of the ground ^3P term in O^{16} in terms of the proton g-factor. The results are: $-g_J(O;{}^3P_1)/g_p=493.4236\pm0.0002$ and $-g_J(O;{}^3P_2)/g_p=493.4022\pm0.0002$, where g_p refers to protons in a cylindrical sample of mineral oil. When combined with $g_J(H;{}^2S_{\frac{1}{2}})/g_p$, measured in analogous experiments on hydrogen, and after inserting the theoretical value of $g_J(H;{}^2S_{\frac{1}{2}})$, the oxygen g-factors are found to be $g_J(O;{}^3P_1)=1.500986\pm0.000002$, $g_J(O;{}^3P_2)=1.500921\pm0.000002$. A discrepancy of 7 parts in 10^6 between these values and corresponding theoretical g-factors can probably be ascribed to inaccuracy of the atomic wave functions used in the theoretical calculations.

I. INTRODUCTION

ATOMIC g-factors of light, many-electron atoms can differ slightly from the simple Landé g-factors for several reasons, the two most important of which are the anomalous spin magnetic moment of the electron and relativistic and diamagnetic contributions to the linear Zeeman energies. A detailed theory of the latter corrections has been developed in recent years,[1–5] but its application to a particular atom is limited by the necessity of having accurate wave functions for the atom. Thus a precisely measured atomic g-factor can be compared meaningfully with theory in one of three different ways, depending on which two of the three theoretical aspects—electron spin moment, relativistic and diamagnetic corrections, atomic wave functions—can be regarded as reliably known. Further complications are added by small theoretical g-factor corrections for deviations from LS coupling and motion of the nucleus, as well as by the experimental fact that only in measuring g-factor ratios can the full precision ($\sim$1 part in 10^6) of modern Zeeman spectroscopy be realized.

As would be expected on the grounds of their accurately known wave functions, measurements on one- and two-electron atoms have provided the best confirmation to date of both the relativistic-diamagnetic g-factor corrections and the quantum electrodynamic prediction of the electron spin moment anomaly. A recent measurement[6] to one part in 10^6 of $g_J(He;{}^3S_1)/g_J(H;{}^2S_{\frac{1}{2}})$, which is essentially independent of the electron spin moment anomaly, is in exact agreement with theory, calculated to order $\alpha^2\mu_0 H$. Measurements[7,8] of $g_J(H;{}^2S_{\frac{1}{2}})/g_p$, where g_p is the proton g-factor, have been used to deduce the value of the electron spin magnetic moment to a precision of several parts in 10^6. The measurement of $g_J(H)/g_p$ is combined with the result of a cyclotron resonance measurement[9,10] of g_p/g_l in order to get finally g_s/g_l, the ratio of the electron spin moment to its orbital moment.

In 1952 Rawson and Beringer,[11] seeking evidence of the electron spin moment anomaly in complex atomic states, measured the g-factors of the ground ^3P term in oxygen. Their results were inconclusive, chiefly because calculations of relativistic-diamagnetic corrections to atomic g-factors had not then been extended beyond the two-electron case. Stimulated by Rawson and Beringer's results, a great deal of effort[3–5] has since then been devoted to the theory of relativistic-diamagnetic corrections for arbitrary complex atoms; special results of this work are precise theoretical g-factors for oxygen.

We have remeasured the oxygen g-factors to a precision of one part in 10^6, with the aim of providing a rigorous test, to order $\alpha^2\mu_0 H$, of the theory of atomic magnetism for a many-electron atom. At present the significance of such a comparison between theory and experiment is obscured somewhat by doubt in the quality of the available atomic wavefunctions. Provided that the uncertainty imposed by wave functions can be removed, and in combination with existing measurements of other atomic g-factors, the results of this experiment can provide a value correct to order α^2 of the fundamental ratio g_s/g_l.

II. THE OXYGEN SPECTRUM

The Zeeman splittings of the ^3P term, calculated with the assumption of pure LS coupling, are shown in Fig. 1. The center part of the diagram represents the linear Zeeman effect; shown on the right are the quadratic level displacements which, at a working field of 4400 gauss, conveniently separate the six transition energies labeled a through f in Fig. 1. Zeeman energies of third order in H vanish for a ^3P term in LS coupling, and

* This work was supported in part by the Office of Naval Research.
† Submitted by H. E. Radford in partial fulfillment of the Ph.D. thesis requirement at Yale University.
‡ General Electric Fellow, 1957–1958.
[1] W. Perl and V. W. Hughes, Phys. Rev. **91**, 842 (1953).
[2] W. Perl, Phys. Rev. **91**, 852 (1953).
[3] A. Abragam and J. H. Van Vleck, Phys. Rev. **92**, 1448 (1953).
[4] K. Kambe and J. H. Van Vleck, Phys. Rev. **96**, 66 (1954).
[5] F. R. Innes and C. W. Ufford, Phys. Rev. **111**, 194 (1958).
[6] Drake, Hughes, Lurio, and White, Phys. Rev. **112**, 1627 (1958).
[7] Koenig, Prodell, and Kusch, Phys. Rev. **88**, 191 (1952).
[8] R. Beringer and M. A. Heald, Phys. Rev. **95**, 1474 (1954).
[9] P. Franken and S. Liebes, Jr., Phys. Rev. **104**, 1197 (1956).
[10] W. A. Hardy, Bull. Am. Phys. Soc. II, 4, 37 (1959); See also Schupp, Pidd, and Crane, Bull. Am. Phys. Soc. II, 4, 250 (1959).
[11] E. B. Rawson and R. Beringer, Phys. Rev. **88**, 677 (1952).

fourth order energies are entirely negligible (less than one part in 10^8) for the purposes of this experiment.

In practice the magnetic field is varied to bring successive transitions into resonance at the frequency of the incident monochromatic radiation. This frequency, a nominal 9105 Mc/sec, was usually changed slightly for each transition. The resonance conditions for $\Delta M=\pm 1$ transitions can then be written as

$$h\nu_a=g_1\mu_0 H_a+AH_a^2, \quad h\nu_b=g_1\mu_0 H_b-AH_b^2, \quad (1)$$

$$h\nu_c=g_2\mu_0 H_c+BH_c^2, \quad h\nu_f=g_2\mu_0 H_f-BH_f^2, \quad (2)$$

$$h\nu_d=g_2\mu_0 H_d+CH_d^2 \quad h\nu_e=g_2\mu_0 H_e-CH_e^2, \quad (3)$$

where A, B, and C are constants depending on the fine structure separations of the three ^3P levels and H_a is the magnetic field required to bring transition a into resonance at frequency ν_a, etc. The predicted six-line spectrum is shown in Fig. 2. Lines corresponding to the three $\Delta M=\pm 2$ ("double quantum") transitions[12] in the $^3P_2$ state are omitted. Normally interspersed between the four $^3P_2$ $\Delta M=\pm 1$ lines, they were unobservable at the low intensity of radiation used in the present work. The assumption of LS coupling can be checked by comparing with the observed oxygen spectrum the quadratic field splittings predicted by (1), (2), and (3). In Table I the mean results of sixteen independent measurements of these field splittings are shown, together with the LS coupling predictions. The agreement is satisfactory, considering possible errors in the measured fine structure separations[13] of Fig. 1.

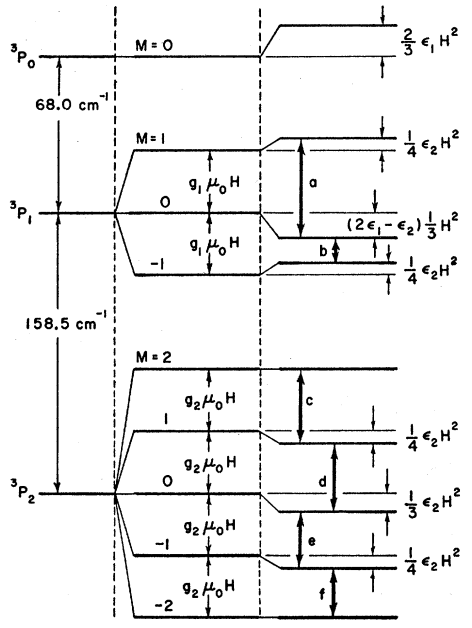

FIG. 1. Magnetic energy levels of the ground ^3P term in oxygen (not to scale). $\epsilon_1=\mu_0^2/(68.0\ hc)$ erg-gauss^{-2}, $\epsilon_2=\mu_0^2/(158.5\ hc)$ erg-gauss^{-2}. Observed lines correspond to transitions labeled a through f.

[12] V. W. Hughes and J. S. Geiger, Phys. Rev. **99**, 1842 (1955).

[13] B. Edlén, Kgl. Svenska. Vetenskapsakad. Handl. **20**, No. 10 (1943). The measured splittings of Table I are in near perfect agreement with LS coupling theory for $^3P_2-{}^3P_1=158.13$ cm^{-1} and $^3P_1-{}^3P_0=68.65$ cm^{-1} [J. J. Hopfield, Phys. Rev. **37**, 160 (1931)].

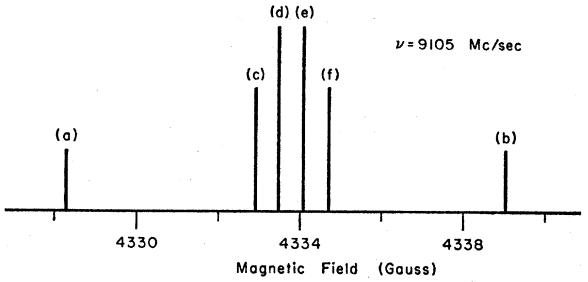

FIG. 2. Schematic representation of the predicted paramagnetic resonance spectrum of atomic oxygen. Lines are labeled to correspond with Fig. 1.

The magnetic field is measured in terms of the proton resonance frequency at that field, given by

$$hf=-g_p\mu_0 H. \quad (4)$$

Substituting (4) into Eqs. (1), for example, and eliminating the constant A gives

$$\frac{g_1}{g_p}=\frac{\nu_a}{f_a}\frac{1+(\nu_b/\nu_a)(f_a/f_b)^2}{1+f_a/f_b},$$

and two similar expressions for g_2/g_p follow from (2) and (3). Thus by combining measurements on pairs of lines, the effect of quadratic field splittings on deduced g-factor ratios can be eliminated.

III. THE EXPERIMENT

1. Apparatus

A description of the Yale paramagnetic resonance absorption spectrometer, developed by Beringer and his students, is given in reference 8. For the present experiment the gas feed system was changed somewhat, and improvements were made in the magnetic field homogeneity and in the spectrometer sensitivity.

Gas system.—A continuous flow method was used because it permits rarified vapors to be studied while maintaining the necessary higher pressure in the atom-producing discharge tube. An electrodeless radio-frequency discharge was found to deliver up to three times as many oxygen atoms to the microwave cavity as the conventional direct-current discharge. To inhibit recombination of the oxygen atoms, the inner wall of the tubing connecting the discharge region with the cavity was

TABLE I. Comparison of measured quadratic field splittings with LS coupling theory.

	Observed[a] (gauss)	Calculated (gauss)
H_b-H_a	10.764 ±0.001	10.88
H_e-H_d	0.6188±0.0005	0.617
H_f-H_c	1.8541±0.0006	1.850

[a] Unweighted mean results of sixteen independent measurements, together with their statistical standard errors.

coated with fused metaphosphoric acid, a treatment that appears to work as well for oxygen as for hydrogen[8] and nitrogen.[14] A thin coating of *SC*-77 Dri-Film[15] accomplished the same purpose, though not as effectively, in the quartz tube which conducted the atomic oxygen vapor through the microwave cavity. Fused metaphosphoric acid when used in this region was found to lower the cavity Q by an objectionable amount.

The discharge tube was fed with ordinary tank oxygen through a glass capillary leak whose conductance could be varied over a wide range by electrically heating the capillary.[16] Oxygen gas was pumped through the system and exhausted to the room by a 7-liter/sec mercury diffusion pump backed by a mechanical pump.

Magnetic field.—The principal source of line broadening in previous work with this apparatus has been inhomogeneities in the magnetic field of 70 milligauss or more over the gas sample volume. In an effort to realize the greater precision and sensitivity that accompany a reduction in line width, the 8-inch electromagnet was mechanically realigned and its pole caps were refinished. Subsequent exploration of the magnetic field in the air gap showed that by suitably placing a small brass shim behind one of the pole caps and then rocking and warping the pole cap on this shim with jacks placed in the air gap, magnetic fields uniform to better than 10 milligauss could be produced over the sample region, a 4-cm^3 cylindrical volume at the center of the air gap.

Maps of the field distribution were made with a traveling proton resonance probe containing a 0.4-cm^3 water sample, while regulating the field with another proton resonance probe. Both proton resonance oscillators were stabilized to 1 part in 10^7 by phase-locking them against the sum of two frequencies, 18.3 Mc/sec from the laboratory frequency standard and 128–154 kc/sec from a BC-221 frequency meter. The same field control and measuring system was used when calibrating the field for an oxygen measurement, except that the traveling probe was replaced by a mineral oil probe designed to fit into the microwave cavity in place of the atom vapor tube. Each time the magnet was turned on, an hour or two of alternate pole cap jacking and field mapping was necessary to get a good field distribution. No oxygen data were taken with fields whose measured inhomogeneity was greater than 15 milligauss over the sample volume.

The field maps were necessarily made with the microwave cavity removed, and slight changes in the field distribution could be expected on inserting the cavity assembly into the air gap. For this reason final trimming of the field was done with small nickel shims after installing the cavity. The best positions of these shims were judged by the amplitude and symmetry of the field calibration proton resonance pattern as displayed on an oscilloscope. As a final check on the field quality before recording microwave absorption data, proton resonance line shapes were observed by slowly sweeping the 30-cps modulated field through the calibrator probe resonance and feeding the absorption signal to a lock-in detector and strip chart recorder. The line shapes were always found to be consistent with the field homogeneity measured before installing the microwave cavity.

The electromagnet was powered by an eight-volt battery of 3000-ampere hour submarine cells. At the 40 amperes required to reach our working fields this provided an exceptionally smooth and stable source of current, and in combination with the proton resonance field regulator gave field stabilities at the regulator probe which depended only on the frequency stability of the proton oscillator, 1 part in 10^7 per hour. Long-term field drifts at the location of the field calibrator probe were typically 5 parts in 10^7 per hour.

Spectrometer sensitivity.—Under good observing conditions the oxygen line widths were 10 ppm measured between peaks of the quasi-derivative line shape. This is one-fourth the width of Rawson and Beringer's[11] lines, and can be attributed to improved field homogeneity and the lower oxygen gas pressures used. This does not translate directly into a fourfold increase in sensitivity; the microwave power level had to be kept much lower to avoid saturation broadening of the low-pressure lines, and it is well known that the efficiency of a barretter detector decreases rapidly with the carrier power level.[17] This was partially offset by constructing special barretters from 35 micro-inch core diameter Wollaston wire. Their noise figures were as much as five times smaller than that of a Sperry model 821 barretter.

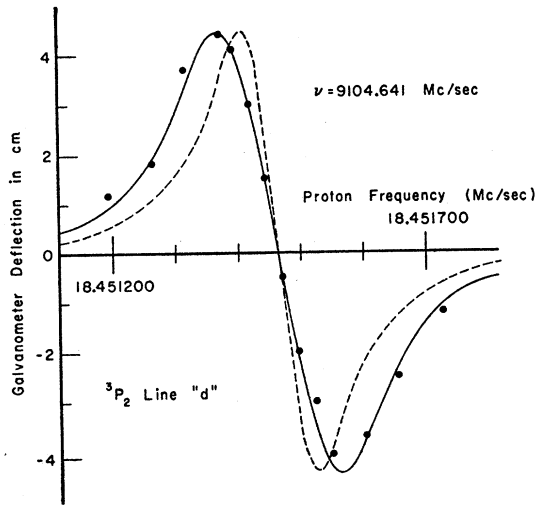

FIG. 3. An observed oxygen line. The solid curve is a theoretical line shape which represents the modulation-broadened derivative of a Lorentz absorption line. The dashed line is the pure derivative of the same Lorentz line; it illustrates the amount of field modulation broadening present.

[14] M. A. Heald and R. Beringer, Phys. Rev. **96**, 645 (1954).

[15] A silicone product of the General Electric Company. It was first used for this purpose by J. P. Wittke and R. H. Dicke, Phys. Rev. **103**, 620 (1956) in their investigation of the hydrogen hyperfine structure.

[16] R. K. Smither, Rev. Sci. Instr. **27**, 964 (1956).

[17] R. Beringer, Ann. N. Y. Acad. Sci. **55**, 814 (1952).

The absolute sensitivity of the apparatus may be defined in terms of a maximum observable absorption Q of the gas sample.[17] For a microwave carrier power of 3×10^{-5} watt, measured at the barretter, the maximum observable Q is 2×10^{8} with the spectrometer in its present state. This represents an increase in sensitivity by a factor of seven over that of a previous experiment[18] performed at the same microwave power level. About 10^{14} oxygen atoms per cm^3 were required to give a conveniently observable (signal-to-noise ratio of 5) absorption line at this microwave power level.

2. Line Shapes and Broadening Mechanisms

Beringer and Castle[19] have shown that a magnetic resonance spectrometer employing field modulation will display the true derivative of the absorption line only for vanishingly small modulation amplitudes. In practice the modulation amplitude must be comparable to the absorption half-width to avoid excessive loss of signal, and this causes a considerable broadening and distortion in the observed line shapes. For observation at the modulation frequency, the expected experimental line shape may be found by calculating the fundamental Fourier component of the signal produced by modulating the field about selected points on the absorption line. Figure 3 shows a fit of such a line shape to a set of experimental data. The absorption line was assumed to have a Lorentz shape, and for comparison its true derivative (dashed curve) is shown.

The observed pressure dependence of the oxygen absorption half-widths is shown in Fig. 4, which combines Geiger's earlier unpublished results with some low-pressure data taken in the present experiment. His lower pressure lines were broadened by magnetic field inhomogeneities. Corrections have been made to all the data to account for field modulation broadening. Operating pressures for the g-factor measurements were chosen by minimizing the observed line width while maintaining a convenient signal amplitude by adjusting the amplitude of field modulation. This led to operating pressures in the range 30–50 microns, definitely in a linear range of the width *vs* pressure curve. We estimate that broadening by magnetic field inhomogeneities and wall collisions cannot account for more than 30 kc/sec of the 100 kc/sec observed absorption half-width at 45 microns. The expected Doppler broadening[20] is negligible, as is the measured saturation broadening.

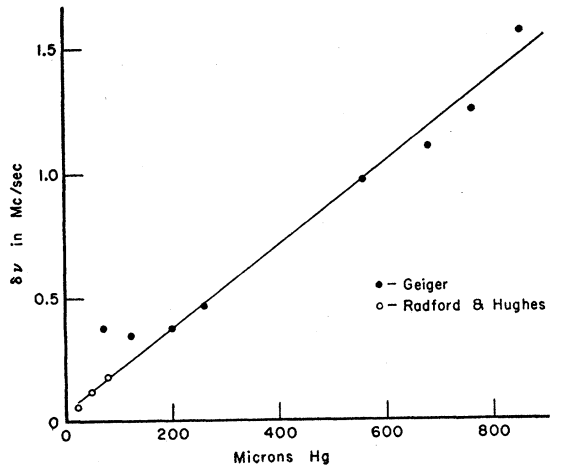

FIG. 4. Dependence of oxygen absorption half-width ($\delta\nu$) on pressure at the microwave cavity. Experimental points were obtained from fits of theoretical line shapes to experimental data, as illustrated by Fig. 3. Field inhomogeneity broadening was significant in Geiger's low-pressure measurements.

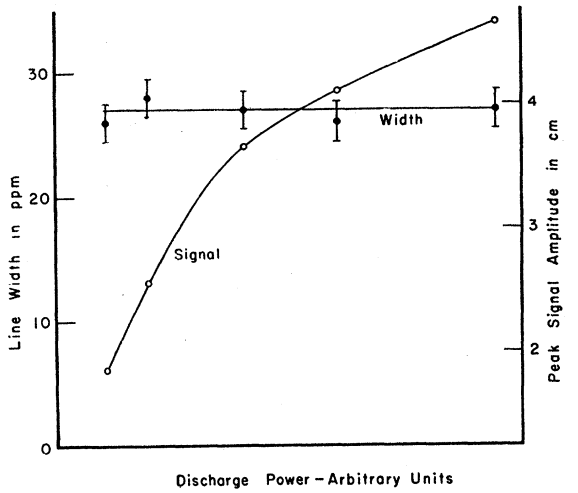

FIG. 5. Illustration of the apparent impotence of atom-atom interactions as causes of line broadening in oxygen. Line width units are parts per million. For further deductions from this figure, see text.

It is clear from Fig. 4 and the foregoing discussion that gas collisions were the chief broadening influence on the oxygen absorption lines. The relative effectiveness of atom-atom and atom-molecule collisions can be investigated by recording line widths while varying the relative atomic and molecular concentrations. The result of one such investigation is shown in Fig. 5. Over a range of radio-frequency discharge power in which the peak absorption signal increased threefold, there was no significant change in line width. The data of Fig. 5 were taken at a pressure of roughly 80 microns Hg; the same behavior was observed at several lower pressures. The experimental conditions were such as to maintain a constant number of atoms, either free or bound into molecules, in the microwave cavity. Provided the extent of molecular dissociation was significant, Fig. 5 then implies that atom-molecule interactions are twice as effective in broadening the oxygen lines as atom-atom interactions.

Atomic concentrations in the microwave cavity can be estimated from measured signal amplitudes. Adapting the analysis of Beringer and Castle[19] to the present

[18] Geiger, Hughes, and Radford, Phys. Rev. **105**, 183 (1957).
[19] R. Beringer and J. G. Castle, Jr., Phys. Rev. **78**, 581 (1950).
[20] R. H. Dicke, Phys. Rev. **89**, 472 (1953).

TABLE II. Sixteen independent determinations of $g_2(d,e)/g_p$. See text for weighting criteria.

Data set	$-g_2(d,e)/g_p$	Weight (%)
1	493.40129	3.5
2	493.40182	2.2
3	493.40185	2.2
4	493.40192	6.0
5	493.40245	4.0
6	493.40304	3.0
7	493.40284	2.9
8	493.40241	8.7
9	493.40222	10.2
10	493.40222	14.2
11	493.40192	10.2
12	493.40241	6.3
13	493.40300	3.9
14	493.40212	7.3
15	493.40143	5.2
16	493.40228	10.2
Unweighted mean:	$-g_2(d,e)/g_p=493.40222\pm0.00013$	
Weighted mean:	$-g_2(d,e)/g_p=493.40219\pm0.00008$	

experiment, we calculate from the data of Fig. 5 that the density of oxygen atoms in the cavity increased from 2.2×10^{14} cm^{-3} to 6.0×10^{14} cm^{-3} as the discharge power was increased. The latter figure corresponds to a 12% molecular dissociation. This is enough to establish that the unchanging line width of Fig. 5 must indeed be a coincidence caused by a special ratio of line broadening cross sections, and not simply caused by low atomic concentrations. Assuming Maxwellian velocity distributions for the atomic and molecular constituents of the oxygen gas sample, two hard-sphere cross sections for line broadening may be computed from the data of Fig. 4 and Fig. 5. They are

$$\sigma(\text{atom-atom})=(5\pm2)\times10^{-16}\text{ cm}^2,$$
$$\sigma(\text{atom-molecule})=(12\pm3)\times10^{-16}\text{ cm}^2.$$

These values are almost completely independent of the calculated atomic concentrations, provided they are large. The quoted uncertainties reflect the difficulty of estimating gas pressures in the microwave cavity. The principal interactions contributing to these cross sections are expected to be electron exchange in atom-atom collisions, and the electric quadrupole and Van der Waals' induced electric dipole interaction for both atomic and molecular collisions. Magnetic dipole interactions are insignificant.[18]

3. Results

Collected in Table II are the results of sixteen independent determinations of the ratio $g_2(d,e)/g_p$ from the oxygen spectrum. These ratios were calculated from the positions of both the d and e line centers according to the formulas of Sec. II. Line e was arbitrarily chosen to provide the quadratic field correction, and therefore uncertainties in $g_2(d,e)/g_p$ are caused chiefly by errors in the line center measurements on line d. The relative importance of three such sources of error—line width, line asymmetries, and magnetic field drift between calibrations—may be assessed for the individual results of Table II, and this leads to the relative weightings shown. Sixteen measurements on lines c and f and seventeen on lines a and b were analyzed in the same way to give values of $g_2(c,f)/g_p$ and $g_1(a,b)/g_p$. Figure 6 is a histogram of the weighted $g_2(d,e)/g_p$ of Table II. A Gaussian curve of the same area and having the rms deviation of the data is superposed.

The maximum deviation of the measured g_J/g_p ratios from the mean is 1.5 ppm, and this can be accounted for by accidental errors in magnetic field measurements and in tuning the klystron to the cavity resonance frequency. Other accidental errors should be negligible. The possibility of a pressure shift of the oxygen lines was investigated by recording the position of a selected line center as a function of pressure in the microwave cavity over the range 20–80 microns Hg; results showed that a pressure shift, if present at all, is less than 4 parts in 10^7 at 40 microns Hg. Nonrandom errors, such as pressure shifts and uncorrected diamagnetic effects, should mostly cancel anyway when the $g_J(\text{O})/g_p$ are combined with other g_J/g_p ratios measured under similar circumstances. For this application we take twice the statistical standard error in the weighted mean values of $g_J(\text{O})/g_p$ as the experimental uncertainty, and our results are

$$-g_1(a,b)/g_p=493.42357\pm0.0018,$$
$$-g_2(c,f)/g_p=493.40220\pm0.0020,$$
$$-g_2(d,e)/g_p=493.40219\pm0.0016,$$

where g_p refers to protons in a cylindrical sample of mineral oil of length to diameter ratio 5/1. The unweighted means differ from these by less than 2 parts in 10^7. The experimental equality of $g_2(c,f)/g_p$ and $g_2(d,e)/g_p$ can be regarded as a check on the accuracy of the formulas used in deriving the g-factor ratios from the oxygen spectrum.

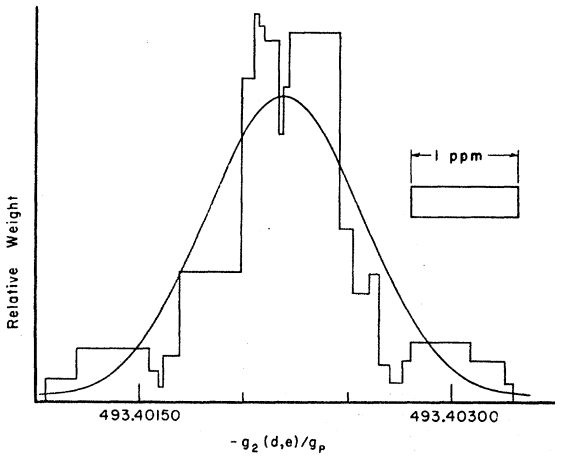

FIG. 6. Histogram of weighted g-factor determinations from the oxygen $^3P_2$ lines d and e. A Gaussian curve of the same area and having the rms deviation of the data is superposed.

These figures may be compared with the primary experimental results[21] of Rawson and Beringer[11]:

$$-g_1(a,b)/g_p=493.4247,$$
$$-g_2(c,f)/g_p=493.4030,$$
$$-g_2(d,e)/g_p=493.4027,$$

which are based on two observations of the oxygen spectrum whose results agreed to 4 ppm.

In order to eliminate the relatively poorly known quantity g_p, we combine our $g_J(\mathrm{O})/g_p$ ratios with the mean of two earlier $g_J(\mathrm{H})/g_p$ measurements: one[8] made with this apparatus and one[7] made by atomic beam spectroscopy. Corrections for shape-dependent diamagnetism of the proton sample must be made to both results; the absorption experiment used a cylindrical mineral oil sample of length to diameter ratio 3/1 and the atomic beam experiment used a spherical mineral oil sample. These corrections can be calculated from experimental measurements of the demagnetization factors of finite diamagnetic cylinders.[22] Taking the magnetic susceptibility of mineral oil as -0.73×10^{-6} cgs emu,[7] the corrections necessary in the $g_J(\mathrm{H})/g_p$ to make them compatible with our $g_J(\mathrm{O})/g_p$ measurements are -0.2 ppm and -1.3 ppm for, respectively, the absorption and atomic beam measurements. The mean of the two adjusted $g_J(\mathrm{H})/g_p$ ratios is $-g_J(\mathrm{H})/g_p=658.2167\pm0.0006$ where the error has been chosen to include both experimental results. Combining this with our $g_J(\mathrm{O})/g_p$ ratios gives

$$g_J(\mathrm{O};{}^3P_1)/g_J(\mathrm{H})=0.7496369\pm0.0000007,$$
$$g_J(\mathrm{O};{}^3P_2)/g_J(\mathrm{H})=0.7496045\pm0.0000007.$$

4. Discussion

We use the theoretical hydrogen g-factor,[23] $g_J(\mathrm{H};{}^2S_{\frac{1}{2}})=g_s(1-\alpha^2/3)$, to convert the $g_J(\mathrm{O})/g_J(\mathrm{H})$ ratios to the $g_J(\mathrm{O})$ form. With $g_s=2(1.0011596)$,[24] the results are

$$\left.\begin{aligned} g_J(\mathrm{O};{}^3P_1)&=1.500986\pm0.000002,\\ g_J(\mathrm{O};{}^3P_2)&=1.500921\pm0.000002.\end{aligned}\right\}\ \text{(experiment)}$$

The theoretical g-factors calculated by Kambe and Van Vleck,[4] with numerical corrections by Innes and Ufford,[5] are

$$\left.\begin{aligned} g_J(\mathrm{O};{}^3P_1)&=1.500996,\\ g_J(\mathrm{O};{}^3P_2)&=1.500932,\end{aligned}\right\}\ \text{(theory)}$$

where the same value of g_s has been used.

Although the absolute values of the experimental and theoretical g-factors differ by some 7 ppm, the differences of the two g-factors agree remarkable well. We therefore look for the source of the discrepancy in theoretical g-factor corrections which are the same for the ${}^3P_1$ and ${}^3P_2$ levels. The largest by far of these corrections is the electron spin moment anomaly, but because of the way it enters both the theoretical oxygen and hydrogen g-factors a change by 20 ppm in g_s/g_l would be required to close the 7 ppm gap in the absolute $g_J(\mathrm{O})$ values. Such a value of g_s/g_l would disagree seriously with earlier measurements[7,8,9,10] of this ratio.

The largest of the relativistic-diamagnetic corrections common to $g_J({}^3P_1)$ and $g_J({}^3P_2)$ is the "relativistic correction proper."[4] It requires accurate knowledge of $\langle T\rangle_{2p}$, the mean kinetic energy of a $2p$ electron. Kambe and Van Vleck calculated $\langle T\rangle_{2p}$ in three different ways within the Hartree-Fock formalism, using the best available Hartree-Fock one-electron wave functions.[25] The results agreed to within 2% but this, as they point out, only provides a check on the accuracy of the one-electron functions; it says nothing about how well the oxygen wave functions are actually represented by linear combinations of products of these one-electron functions. The answer to this question can be sought in comparisons of the observed energies of the oxygen atom with those calculated from the one-electron functions. The calculated spin-orbit parameter, for instance, is 10% too high.[4] On the other hand, the ratio of calculated intermultiplet splittings $({}^1D-{}^1S)/({}^3P-{}^1D)$ agrees to within 1% with experiment.[25] Perhaps most significant for our purposes is a comparison of calculated and observed ionization energies: the difference here is 25%.[25] Since only a 5% change in the mean kinetic energy $\langle T\rangle_{2p}$ would make both theoretical oxygen g-factors agree perfectly with experiment, we believe there is no need to look further for the cause of the 7 ppm discrepancy—very probably the blame lies with the Schroedinger wave functions used in calculating the relativistic-diamagnetic g-factor corrections.

Note added in proof.—Several of the one- and two-electron integrals involved in the theoretical oxygen g-factors have been recalculated recently by Freeman.[26] The same wave functions[25] were used, but great care was taken to exclude errors originating in the numerical integrations. These results, inserted wherever possible in the theoretical g-factor expressions, reduce both of the numerical values listed above by 1 ppm. The discrepancy between theory and experiment is thus reduced to 6 ppm.

[21] The quoted $g_J(\mathrm{O})$ values of reference 11 are gotten by multiplying $g_J(\mathrm{O})/g_p$ by $g_p=g_s/(g_s/g_p)=2(1.0011454)/658.2271$. We have converted these back to the $g_J(\mathrm{O})/g_p$ form.

[22] W. C. Dickinson, Phys. Rev. **81**, 717 (1951).

[23] G. Breit, Nature **122**, 649 (1928).

[24] C. M. Sommerfield, Ann. Phys. (N. Y.) **5**, 26 (1958).

[25] Hartree, Hartree, and Swirles, Trans. Roy. Soc. London **A238**, 229 (1939).

[26] A. J. Freeman, Ordnance Materials Research Laboratory Report No. 28, June 1957; A. J. Freeman and P. O. Löwdin, Phys. Rev. **111**, 1212 (1958); A. J. Freeman, J. Chem. Phys. **28**, 230 (1958).